An Apoptotic Model for Nitrosative Stress†

Jerry P. Eu,‡ Limin Liu,§ Ming Zeng,‡ and Jonathan S. Stamler*,‡,§

Department of Medicine and Howard Hughes Medical Institute, Duke University Medical Center, Durham, North Carolina 27710

Received August 31, 1999; Revised Manuscript Received November 17, 1999

ABSTRACT: Nitric oxide overproduction has been implicated in the pathogenesis of many disorders, including artherosclerosis, neurodegenerative diseases, inflammatory and autoimmune diseases, and cancer. The common view holds that nitric oxide-induced cellular injury is caused by oxidative stress. This theory predicts that interactions between reactive nitrogen species and reactive oxygen species produce powerful oxidants that initiate cell death programs. Cytokine-treated murine macrophages are the prototype of this form of cellular injury. Here we report that generation of reactive nitrogen species upon lipopolysacharide/interferon-γ stimulation of RAW 264.7 cells is largely divorced from production of reactive oxygen species, and that oxidative stress is not principally responsible for cell death (in this model). Rather, the death program is induced mainly by a nitrosative challenge, characterized by the accrual of nitrosylated proteins without a major alteration in cellular redox state. Moreover, interactions between reactive oxygen and nitrogen species may alter the balance between pathways that yield nitrite and nitrate, without impacting the level of S-nitrosylation or extent of cell death. Our results thus (1) provide new insights into NO-related metabolic pathways, (2) demonstrate that apoptotic injury can be caused by nitrosative mechanisms, and (3) establish a model for nitrosative stress in mammalian cells.

Stimulation of cells with lipopolysaccharide (LPS)[1] and interferon-γ (INF-γ) leads to induction of type 2 nitric oxide synthase (iNOS) and generation of reactive nitrogen species (RNS) (*1*). This pathway has been implicated in apoptosis (that is partly p53-dependent) (*2*−*11*), and thus in the pathogenesis of multiple disorders, including atherosclerosis, transplant rejection, heart failure, neurodegenerative disorders, inflammatory diseases, septic shock, and cancer. Cytokine stimulation also generates reactive oxygen species (ROS) (*12*−*16*), which may contribute to cell demise (*12*−*22*). Indeed, current opinion holds that ROS may execute the death program in p53-expressing cells (*13*, *17*−*19*), and that interactions between RNS and ROS promote the apoptotic process by generating powerful oxidants (*12*, *15*, *16*, *23*).

In point of fact, the role of oxidants in apoptosis is poorly understood. It is not clear if ROS serve principally as downstream effectors (*18*, *20*, *24*, *25*) or upstream transducers (*17*, *20*, *26*, *27*) of apoptotic signals, and there are even indications for protective roles (*3*, *27*−*29*). It is also not known if ROS act alone or synergistically with RNS (*24*, *27*, *29*). In particular, reactive nitrogen and oxygen species may be generated at different times in a cellular response or at different loci within the cell (*30*−*32*). This combination of events could determine the identity of the NO- or O_2-related signal and its functional consequences. Very little is known, however, of the spatial and temporal regulation of RNS and ROS or of the molecular basis of redox responsiveness in apoptotic programs.

Chemical and spectroscopic analyses have revealed that RNS can nitrosylate cysteine and transition metal centers in proteins; that is, NO can attach covalently (or coordinately) to redox centers without causing oxidation (*33*−*35*). Such posttranslational modification has been widely implicated in control of both cellular and system functions, including respiration, neuronal plasticity, vasorelaxation, skeletal muscle contractility (excitation−contraction coupling), immunity, and apoptosis (*6*, *33*, *34*, *36*−*39*). The picture that has emerged from these studies indicates that nitros(yl)ation is generally utilized as a reversible signal in biological reactions (*33*−*35*). But recent work in prokaryotes is revealing that nitrosylation can also exceed a dangerous threshold, thereby constituting a cellular threat (*40*). In such cases, the organism counters with a defense that detoxifies nitrosants and otherwise lowers the level of nitrosylation. By analogy, one might speculate that nitrosylation can function as a stress in eukaryotes. However, this view has not been fully embraced due to the belief that a concomitant production of ROS, such as superoxide, would favor the alternative NO reaction pathway to peroxynitrite and/or its elimination as nitrate, and that intracellular glutathione would prevent any significant endogenous nitrosylation of proteins.

Here we report that induction of iNOS in murine macrophages produces a nitrosative stress that is, in significant part, temporally divorced from the oxidative respiratory burst

† This work was supported by grants (HL52529 and HL59130) from the NHLBI.

* Address correspondence to this author at HHMI, Duke University Medical Center, Box 2612, Durham, NC 27710. Telephone: (919) 684-6933. Fax: (919) 684-6998. Email: staml001@mc.duke.edu.

‡ Department of Medicine.

§ Howard Hughes Medical Institute.

[1] Abbreviations: LPS, lipopolysaccharide; INF-γ, interferon-γ; NOS, nitric oxide synthase; RNS, reactive nitrogen species; SNO, *S*-nitrosothiols; GSNO, *S*-nitrosoglutathione; GSH, reduced glutathione; GSSG, oxidized glutathione; AEBSF, 4-(2-aminoethyl)benzenesulfonyl fluoride; L-NMMA, N^G-monomethyl-L-arginine; L-NIO, L-N^G-(1-iminoethyl)-L-ornithine; mBrB, monobromobimane; DAN, 2,3-diaminonaphthalene; DCF-DA, 2′,7′-dichlorofluorescein diacetate.

10.1021/bi992046e CCC: $19.00
Published on Web 01/11/2000

and primarily responsible for initiating the apoptotic program. This model system may be useful for elucidating the biochemical and genetic basis of NO responsiveness and the molecular mechanisms underlying programmed cell death.

METHODS

Materials. RAW 264.7 cells were purchased from American Tissue and Cell Culture. Reduced glutathione (GSH), oxidized glutathione (GSSG), glutathione reductase (GR), sodium pyruvate, NADPH, NADH, nitrate reductase (*Aspergillus*), sulfanilamide, *N*-(1-naphthyl)ethylenediamine (NED), *p*-chloromercuribenzosulfonic acid (PCMBS), perpropidium iodide, 5-amino-2,3-dihydro-1,4-phthalazinedione (Luminol), 4-(2-aminoethyl)benzenesulfonyl fluoride (AEB-SF), and LPS (*E. coli* serotype 0128:B12) were purchased from Sigma Chemical. 2′,7′-Dichlorofluorescein diacetate (DCF-DA) was purchased from Acros Organics. 2-Vinylpyridine was purchased from Aldrich Chemical. N^G-Monomethyl-L-arginine (L-NMMA) and monobromobimane (mBrB) were purchased from Calbiochem. L-N^G-(1-Iminoethyl)-L-ornithine (L-NIO) was purchased from Alexis Biochemicals. Phenol-red-free Dulbecco's modified Eagle's media (DMEM) supplemented with pyruvate and L-glutamine, fetal bovine serum (FBS), murine INF-γ, phenol/chloroform/isoamyl alcohol, and penicillin/streptomycin were purchased from Gibco Life Sciences. Sephadex G-25 resin was purchased from Pharmacia. Sodium nitrite was purchased from Mallinckrodtft Chemical. GSNO was made immediately before use by the method described in ref *41*.

Cell Culture and Viability. RAW 264.7 cells (6.5×10^6) were suspended in fresh DMEM supplemented with 10% FBS and 1% streptomycin/penicillin and seeded onto 6-well tissue plates (5 mL per well) 10−12 h prior to stimulation. Cells were allowed to grow to near-confluence in air supplemented with 5% CO_2 at 37 °C. The medium was then replaced, and LPS (100 ng/mL) and murine INF-γ (100 units/mL) or other specified treatments were added. The control group received only replacement of media. Viable cells were counted under a light microscope using trypan blue exclusion criteria, and numbers were verified with a Coulter counter.

Nitrite and Nitrate Levels. Medium was removed from each well, diluted 2-fold with H_2O, and mixed sequentially with an equal volume of 1% sulfanilamide and 0.02% NED (0.5 M HCl) in a 96-well microplate (*41*). The absorbance at 540 nm was then measured using a microplate reader (Molecular Devices), and the nitrite concentrations were derived from standard curves. The nitrate concentration was determined following reduction of nitrate to nitrite (*42*) with nitrate reductase (1 unit/mL) for 1 h in 100 mM Na_2PO_4, 10 mM NADPH, and 0.02 μM FAD (pH 7.4). Rates of nitrite production were also measured in some experiments using 2,3-diaminonaphthalene (below).

Nitrosation Assay (2,3-Diaminonaphthalene). The measurement of macrophage nitrosating activity is based on the formation of a fluorescent triazole derivative at physiologic pH. For this anlaysis, we modified methods of both Misko et al. (*43*) and Andrew et al. (*44*). Briefly, 2×10^6 RAW 264.7 cells were incubated for 1 h (at selected time points following cytokine stimulation) in 1 mL of 20 mM Bis-Tris propane, 130 mM NaCl, and 200 μM 2,3-diaminonaphthalene (DAN) (0.2% *N*,*N*-dimethylformamide), pH 7.0. The supernatant was collected following centrifugation and brought to pH >12 with NaOH. The fluorescent emission spectrum between 400 and 410 nm (excitation at 365 nm) gave optimum sensitivity and was inhibited by L-NMMA. Unstimulated cells were used to obtain the base line. Standard curves were generated using acidified nitrite, after which samples were alkalinized as described above. The nitrite measurement using DAN is based on the formation of a fluorescent signal upon acidification (*43*). Specifically, nitrite only produces a signal upon acidification whereas other nitrosants generate signals at physiologic pH.

Intracellular Nitrosylation. Cell pellets (harvested from 2.5 mL of cell suspension as described under Glutathione Assays below) were lysed in 500 μL of 25 mM Na_2HPO_4 (pH 7.4) with 0.5 mM EDTA and 0.02% Triton X-100 (lysing buffer). The lysate was further sonicated for 20 s before centrifugation at 14000*g* to remove insoluble debris. Paired supernatant aliquots from each sample—one of which was pretreated with 0.375 mM $HgCl_2$ for 10 min to deplete *S*-nitrosothiols (SNOs)—were then assayed for NO using photolysis/chemiluminescence (*41*). Comparable results were obtained when PCMBS (3.75 mM), a more thiol/SNO-selective organic mercurial, was substituted for $HgCl_2$. The NO signals in paired injections were normalized for protein concentration as determined by the Coomassie blue method according to the manufacturer's instruction (Pierce Scientific, Rockford, IL). Additional lysates were passed through G-25 Sephadex columns (MW cutoff = 3000) preequilibrated with lysing buffer in order to determine the protein and low-mass NO fractions. *Nitrosylated peptides and protein* (X-NO) (where X is cysteine, transition metal, or amine) were defined as the total NO signal generated by photolysis. *S-Nitro(so)-thiols (SNOs)* were defined as the component of the NO signal that was eliminated by $HgCl_2$ and PCMBS treatment. *Protein SNOs* were defined as the SNOs in lysates that survived desalting. *Low-mass SNOs including S-nitrosoglutathione (GSNO)* were defined as the SNO content of lysates, which was lost on desalting (the presence of GSNO in the low-mass fraction was verified by anion exchange chromatography).

Protein Thiol. Intracellular protein free thiol content was determined with a modified fluorescence method described by Kosowser and Kosower (*45*). Briefly, 100 μL of lysate was passed through G-25 Sephadex columns and treated with 50 μM monobromobimane (mBrB) (a lipophilic fluorescence probe) for 90 min at room temperature while being protected from light. After subtraction of the base line fluorescence, the intensity at 482 nm (excitation = 382 nm, Perkins-Elmer LS 2B Luminescence Spectrometer) in each sample was converted to the concentration of protein thiol using a calibration curve generated by adding known amounts of glutathione-conjugated fluorescent bimane to the cuvette. Control experiments showed that SNOs did not react with mBrB.

Glutathione Assays. Intracellular total glutathione (GSSG+GSH) and the glutathione disulfide (GSSG) fraction were determined using a microplate recycling assay modified from Griffith (*46*). At different time points, the RAW 264.7 cells in each well were washed twice with PBS, gently scraped off the culture plate, and then suspended in 5 mL of PBS. The cell suspension from each well was counted and divided into two equal halves (one for assay of GSH+GSSG

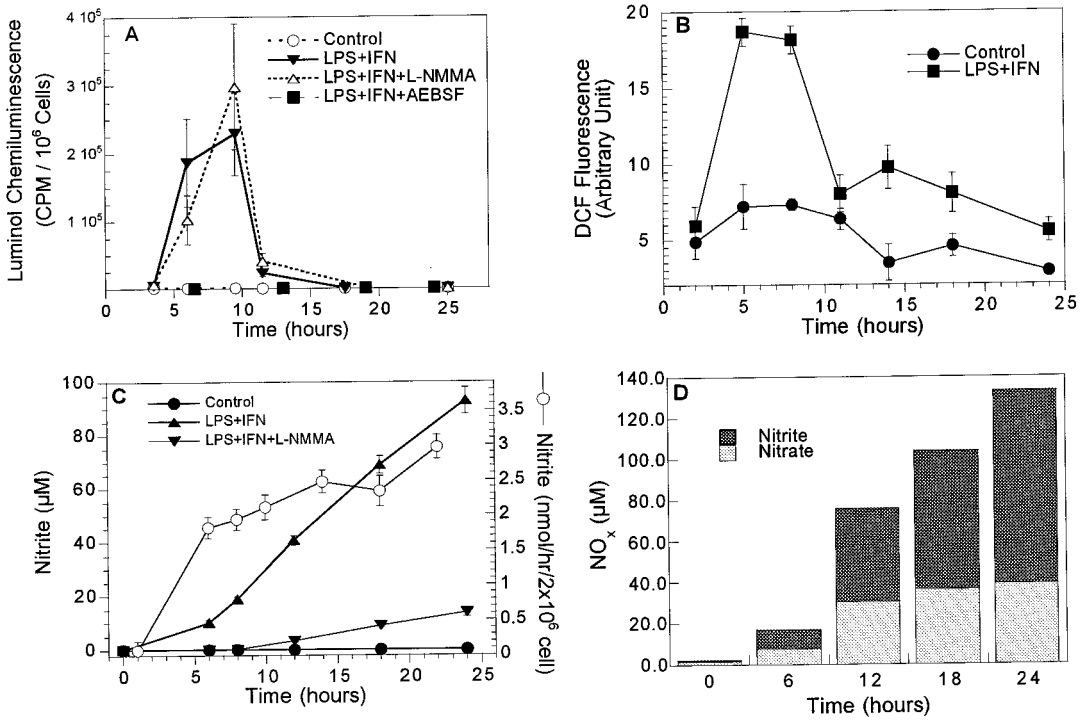

FIGURE 1: Generation of ROS and RNS by cytokine-activated macrophages. (A, B) The production of ROS (respiratory burst) peaks at ~6 h and is complete by about hour 12. ROS generation is inhibited by AEBSF (NADPH oxidase inhibitor) but not by L-NMMA (NOS inhibitor). (C) RNS (nitrite) is detected by hour 6 (closed triangles; measured by Greiss assay) and accumulates at increasing rates (open circles; measured with DAN) thereafter; nitrite production is inhibited by L-NMMA but not by AEBSF (not shown). (D) The ratio of nitrite to nitrate (NO_2^-/NO_3^-) increases from hour 6 (~1:1) to hour 24 (~3:1). Data are the mean ± SEM of 6−10 experiments at each point.

and one for intracellular *S*-nitrosothiol determination) and then centrifuged at 800*g* for 5 min. For the GSH+GSSG assay, cell pellets were lysed in 250 μL of 2.4% perchloric acid, 0.5 mM EDTA, to which 10% sulfosalicyclic acid was added. The cell lysates were subsequently sonicated for 20 s, and centrifuged at 14000*g* for 10 min. The supernatants were then assayed immediately for total glutathione. To determine the oxidized GSSG fraction, reduced GSH was first derivatized with 2-vinylpyridine (2-VP) for 40 min (following neutralization of samples with triethanolamine) (*46*). Control experiments were done to ensure that neither GSNO (up to 10 μM) nor any other inhibitor in the lysate interfered with the assay.

Apoptosis. (A) Nuclear Morphology. Cells were fixed in culture wells with methanol and glacial acetic acid for 3−4 min, and then washed twice with PBS. One milliliter of propidium iodide (PI) (60 μg/mL) and RNase A (300 μg/mL) was added in DMEM and left at 37 °C for 30 min. The stained nuclei were visualized using a fluorescence microscope (Olympus Instruments, model T0401). Photographs (400×) were taken from randomly selected areas. Condensed, fragmented nuclei of nonoverlapping cells (at least 150 nuclei) were counted in each photograph. The results were expressed as the percentage of apoptotic nuclei to total nuclei.

(B) Annexin Binding. Cells were harvested, and apoptosis was determined by FACS analysis (B.D.) using annexin V−FITC and propidium iodine according to the manufacturer's instructions (Calbiochem). Cell Quest software (B.D.) was used to analyze 10 000 gated events. Viable cells were identified by their ability to exclude annexin and PI.

(C) DNA Gel Electrophoresis. We used a method described by Messmer et al. (*4, 6*) to isolate DNA fragments. Electrophoresis were performed using a Phast-Gel system (Pharmacia Biotech): 1.8 μg of DNA was loaded onto each lane of a PhastGel Homogeneous 12.5 and stained with a PhastGel DNA Silver Staining Kit, according to the manufacturer's instructions. The purity and the concentration of the DNA fragments were determined by UV absorbance (260 nm:280 nm) (Perkin-Elmer Lambda 2S UV Spectrometer).

Necrosis. Ten microliters of cell-free medium was taken from each well and assayed, at various time points, for LDH activity by incubation at 30 °C with 125 μL of 10 mM pyruvate and 0.1 mM NADH in 0.081 M Tris, pH 7.2. NADH oxidation was monitored at 340 nm (*47*).

Detection of Reactive Oxygen Species. (A) Luminol Chemiluminesence. RAW 264.7 cells were scraped from their wells in 5 mL of medium. Two milliliters of the cell suspension was then loaded into scintillation vials containing 3 mL of warmed medium. Immediately before reading, 50 μM luminol (final concentration) was added to each vial and shaken gently. Vials were counted for 1 min (Beckman Multipurpose Scintillation 6500 Counter) (*48*).

(B) DCF-DA Assay. DCF-DA was dissolved in 95% EtOH and then diluted with culture medium; 100 μM (final concentration) DCF-DA was added to wells 2 h prior to cell harvest. At the time of assay, the cells in each well were washed once and suspended in 5 mL of PBS. Then 0.5 mL of cell suspension from each well was diluted with 2.5 mL of PBS in a cuvette and the emission fluorescence intensity (FI) taken at 520 nm using an excitation wavelength of 488 nm (Perkins-Elmer LS50B Luminescence Spectrometer) (*49*).

RESULTS

RNS and ROS. The addition of LPS (100 ng/mL) and INF-γ (100 units/mL) to the media of RAW 264.7 cells led

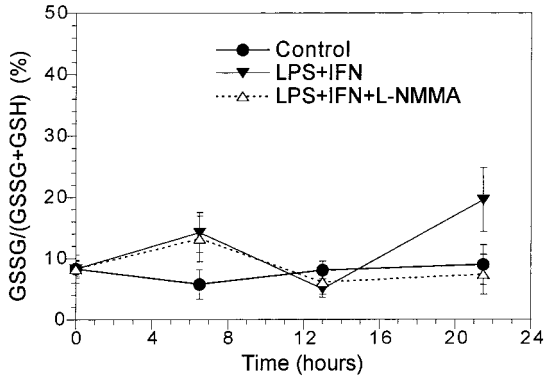

FIGURE 2: Intracellular redox state. Redox state [GSSG/(GSH+GSSG)] was not significantly perturbed by cytokine stimulation nor affected by NOS inhibition (L-NMMA). Data are the mean ± SEM of 6−8 experiments at each point.

to a rapid respiratory burst (detectable at or shortly after our first assay time point of 2 h). ROS generation (*48*, *49*) increased rapidly, peaked at hour 6−9, and normalized by hour 12 (Figure 1A,B). By contrast, RNS accumulated steadily in the media from hour 6 to 24 (Figure 1C). The ratio of nitrite (NO_2^-) to nitrate (NO_3^-) increased from ∼1:1 at the early time points to ∼3:1 at 24 h (Figure 1D). Moreover, the hourly rate of nitrite production increased by ∼70% between hours 6 and 24 (Figure 1C). The NOS inhibitor L-NMMA (1 mM) markedly reduced NO_x^- accumulation, but did not prevent ROS generation (Figure 1A). Conversely, the respiratory burst oxidase inhibitor AEBSF (125 μM) virtually eliminated ROS production (Figure 1A) but had no significant effect on RNS (Figure 3E, and not shown). More specifically, AEBSF reduced NO_x^- levels by ∼20% in some experiments (see below), but the effect did not reach statistical significance. RNS and ROS were barely detectable in the control groups.

Redox State. The ratio of intracellular oxidized glutathione (GSSG) to total glutathione (GSSG+GSH) was used as a measure of intracellular redox state (oxidative stress). Small increases in GSSG were detected at some time points following cytokine treatment. However, the GSSG/GSSG+GSH ratio was not significantly different in the cytokine-treated group from the control group at any time point nor was it affected by addition of L-NMMA (Figure 2; note we use SEM). In addition, GSH/GSSG did not accumulate in the extracellular medium (not shown). Thus, cytokine stimulation of murine macrophages does not result in a major perturbation of cellular redox state under these conditions.

Nitros(yl)ation. N-Nitrosation (N-NO) of 2,3-diaminonaphthalene at pH 7.0 was used as a marker of nitrosative stress. Nitrosation was observed coincident with detection of RNS (Figures 1C and 3A). The rate of DAN nitrosation increased from hour 6 to hour 18 and was sustained throughout the 24 h period of observation (Figure 3A). Nitrosylated cellular constituents were also readily detected throughout the 24 h period. A low constitutive reservoir of nitrosylated protein was present in unstimulated cells, the levels of which were increased ∼10-fold by treatment with cytokines (Figure 3B). Contrary to our expectation, the majority of *S*-nitrosothiol was found to be in protein form. At no time point did low-mass SNOs, including GSNO, constitute more than 25% of the total intracellular pool, and they could not be reliably detected at some time points (Figure 3C). Whereas the rates of nitrite production (Figure 1C,D) and N-nitrosation (Figure 3A) tended to increase

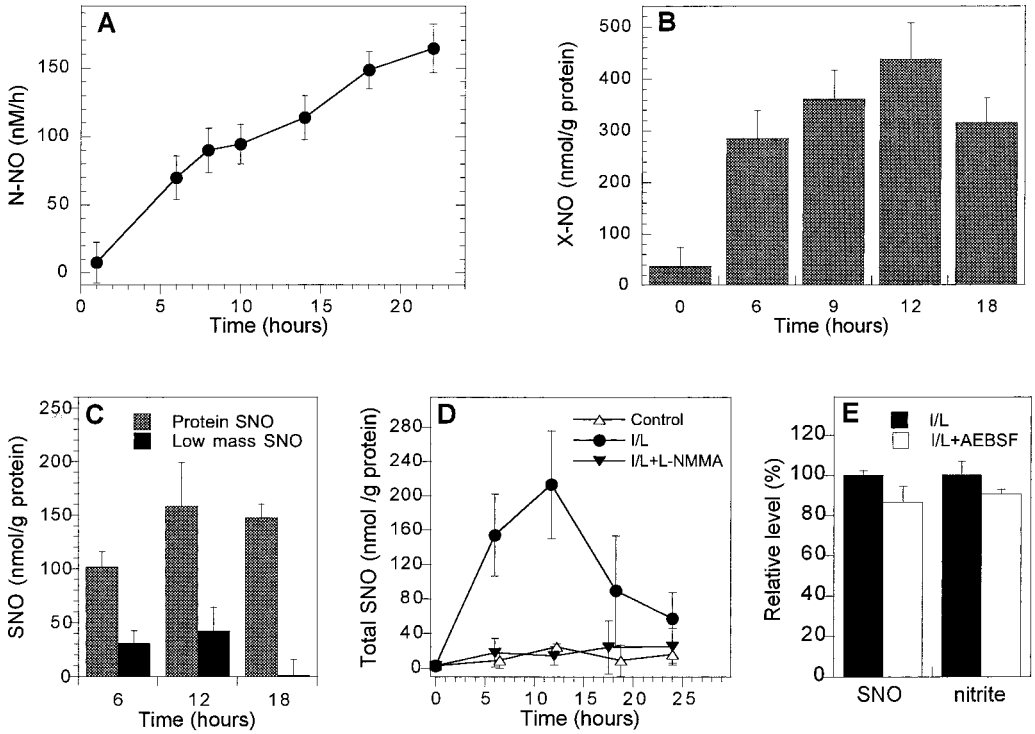

FIGURE 3: Nitrosative stress in cytokine-activated macrophages. (A) Nitrosation of DAN (N-nitrosation) (at pH 7.0) is first detected at hour 6; the rate of N-nitrosation increases throughout the 24 h period. (B) Nitrosylation of intracellular peptides and proteins increases over the first 12 h. (C) Levels of intracellular *S*-nitrosoprotein and low-mass *S*-nitrosothiol following cytokine stimulation are relatively constant (differences do not reach statistical significance). (D) Nitrosative stress (nitrosylation) is blocked by L-NMMA. (E) Nitrosative stress (S-nitrosylation and nitrite generation) is not prevented by AEBSF (12 h incubation). Data are the mean ± SEM of 3−6 experiments at each point. (B−E). Nitrosylation was measured by photolysis−chemiluminesence, as described under Methods.

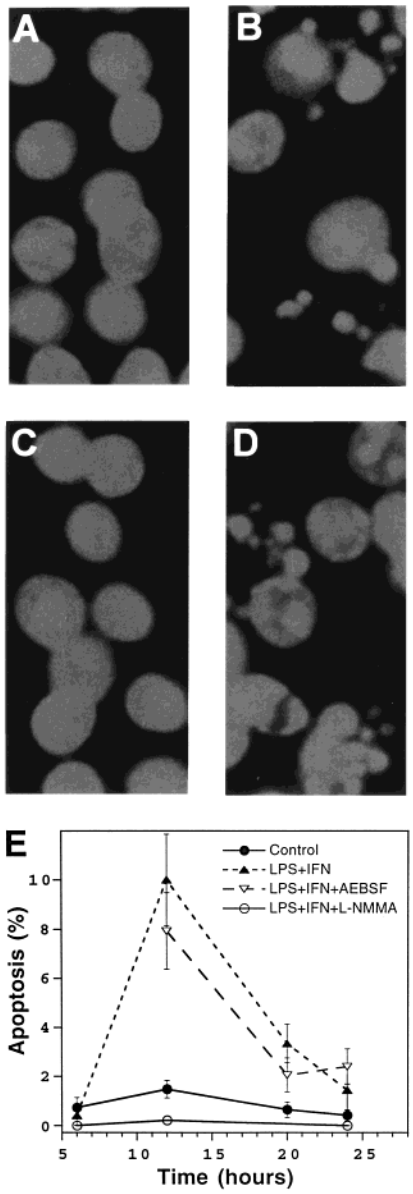

FIGURE 4: Apoptosis assayed by nuclear condensation and fragmentation in LPS/IFN-γ-activated macrophages. Apoptosis is blocked by inhibition of NOS, but not by inhibition of the respiratory burst oxidase. (A−D) Representative pictures of cells stained by propidium iodine: following no treatment (A); treatment with LPS/IFN-γ alone (B); LPS/IFN-γ + L-NMMA (C); and LPS/IFN-γ + AEBSF (D). (E) Combined data (mean ± SEM; % of total cells) are from of 6−18 experiments at each time point.

progressively, S-nitrosylated protein levels rapidly approached a steady state (Figure 3C), during which approximately 1% of bimane-reactive protein thiols were modified. The nitros(yl)ation of DAN (not shown) and/or cellular proteins was inhibited by L-NMMA (Figure 3D) but not by AEBSF (Figure 3E).

Cytotoxicity. Treatment of cells with cytokines resulted in apoptosis as revealed by nuclear morphology (Figure 4), annexin binding (Figure 5), and DNA fragmentation assays (not shown). LDH leakage, indicative of necrosis, was not increased (not shown). The apoptotic process was first visualized 12 h after the addition of cytokines—thus occurring coincident with protein nitrosylation (Figure 3B)—and proceeded for more than 24 h (Figure 4E). Quantitative assessments of apoptosis by fluorescence microscopy (nuclear morphology) and FACS (annexin binding) revealed comparable results, with the exception that early apoptotic cell number (Figure 5) did not decline at 24 h to the extent suggested by nuclear staining (Figure 4E). L-NMMA (1 mM) (but not D-NMMA) markedly protected the macrophages from programmed cell death [$p < 0.005$ for both annexin binding (Figure 5) and nuclear morphology (Figure 4)] over the entire 24 h observation period. The NOS inhibitor L-NIO also inhibited apoptosis (data not shown). In contrast, AEBSF (125 μM) afforded little protection (Figures 4 and 5). Specifically, AEBSF caused a statistically insignificant trend toward reduction in apoptosis (20−30%) as revealed by nuclear staining (Figure 4E) and annexin binding ($p > 0.19$; $n = 6$ for both), the interpretation of which was confounded by a comparable (~20%) reduction in NO_x^- accumulation in some experiments. Neither AEBSF nor L-NMMA alone increased apoptotic cell number above control levels (~1.0%). L-Arginine supplementation (2 mM) had a slight proapoptotic effect on cytokine-treated cells (not shown). Thus, induction of apoptotic cell death is mainly dependent on RNS.

Propidium iodide staining also revealed differences in the number of mitotic nuclei between the groups, consistent with an additional cytostatic action of cytokines (data not shown).

Nitrosant-Induced Apoptosis. Addition of GSNO (for 6 h) to unstimulated macrophages resulted in S-nitrosylation of intracellular constituents and induction of apoptosis (Figure 6). These effects of high micromolar GSNO concentrations closely mimicked those of cytokines in several ways: (1) the lag phase between addition of GSNO and initiation of apoptosis was similar in duration to the lag between RNS generation and cytokine-induced cell death (that is, ~6 h); (2) the amount of apoptosis induced by GSNO (Figure 6A) was comparable to that produced by cytokines; (3) the concentration of intracellular *S*-nitrosoprotein generated by addition of GSNO (Figure 6B) was similar to the concentration produced in cytokine-stimulated macrophages undergoing comparable degrees of apoptosis (Figure 3C); and (4) GSNO did not produce a major oxidative stress (not shown).

DISCUSSION

The identification of NO with oxidant injury has been well-validated (*12*, *23*, *35*, *50*). However, the functional linkage between oxidation and damage is poorly established in most biological systems (*51*−*54*). The problem is well illustrated in models of cytokine-induced apoptosis where redox targets have not been identified or characterized. The new results suggest an alternative model for apoptosis in which the death program is at least partly triggered by nitrosative modifications. That is, nitros(yl)ation is probably the posttranslational modification which provokes the cellular response (in this case). By contrast, oxidation appears to be more associative than causative in this cellular control mechanism. Our studies thus establish that nitros(yl)ation can serve as the molecular basis of a mammalian stress response.

Apoptosis induced by iNOS generally occurs in a minor population of cells (10% in this study; range 5−30%) (*2*−*11*). A similar degree of apoptosis is caused by the NADPH oxidase in human leukemic cells (*55*). These two enzymes have important signaling or other roles unrelated to apoptosis. That is, induction of apoptosis is not the principal function

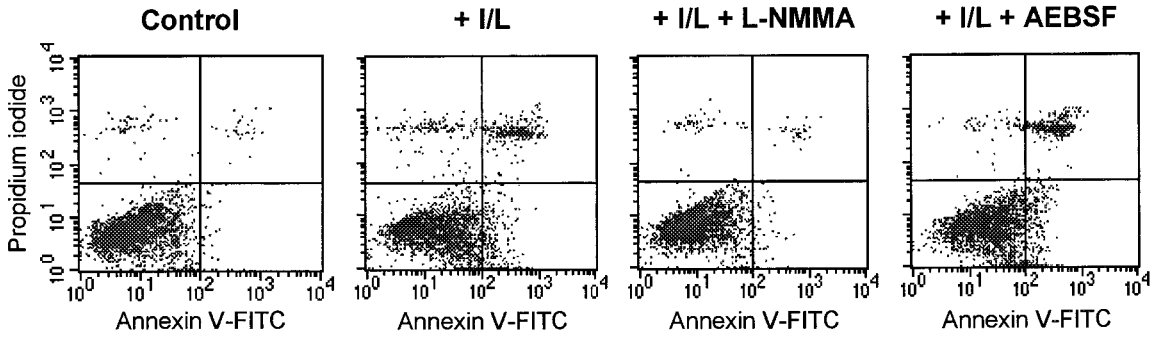

FIGURE 5: Apoptosis assayed by annexin V binding in cytokine-activated macrophages. RAW 264.7 cells untreated (Control) or treated for 12 h with IFN-γ/LPS, IFN-γ/LPS + L-NMMA, or IFN-γ/LPS + AEBSF were assayed for annexin V−FITC and PI staining by FACS. Shown are the data from one representative set of experiments. Four to six independent experiments were performed for each treatment.

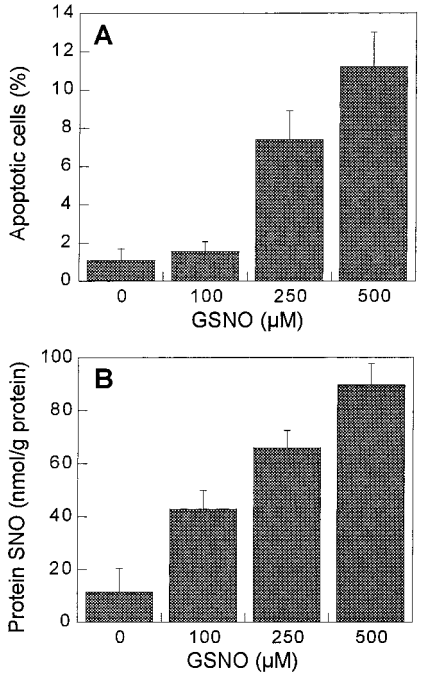

FIGURE 6: Nitrosant-induced apoptosis. Treatment of cells with GSNO leads to apoptosis (A) and accumulation of intracellular S-nitrosylated proteins (B). Levels of nitrosylated protein and apoptosis (determined by nuclear morphology) correlate well with those measured following cytokine stimulation in Figures 3C and 4, respectively. Data are the mean ± SEM of 3−6 experiments at each time point.

of these NADPH-dependent oxido-reductases, rather an inevitable consequence of a high level of activity, and perhaps a reflection of some dysregulation in signal transduction cascades. Nitrosant and oxidant stress responses produced by NADPH-dependent flavohemoproteins thus differ from Fas and nutrient withdrawal, which are primary apoptotic signals and typically kill a majority of cells.

Multiple lines of evidence argue against a primary effector role of ROS in this model of apoptotic injury. First, superoxide/ROS have been shown to safeguard against the injury caused by RNS/NO (*29*) (*56*), a finding in keeping with protection by ROS in some models of Fas-induced apoptosis (*28*) and the view that ROS can be employed to signal the induction of host defenses (*27*). Second, nitration of proteins—which has been viewed as evidence for interactions between ROS and RNS—is not responsible for cell death in this system (*56*). Third, neither cytokine-induced nor GSNO-mediated apoptosis is preceded by a major change in redox state. In this respect, LPS/IFN-γ-mediated apoptosis in macrophages is different from Fas-induced apoptosis in Jurkat T cells (*57*, *58*) or thapsigargin- or dexamethasone-induced apoptosis in thymocytes (*59*). Fourth, and most importantly, blockade of ROS generation by the major cellular oxidase affords little protection from cell death. Although this reasoning does not exclude participation of some ROS in apoptosis, such as those which might be released locally from mitochondria, it argues against primary involvement of oxidant mechanisms in the process.

In contrast, apoptosis is critically dependent on induction of iNOS and well accounted for by nitrosative mechanisms. Specifically: cell death is associated with increased amounts of nitrosylation; RAW cells die when exposed to NO donors that increase levels of protein *S*-nitrosothiol; and blocking nitrosylation with L-NMMA affords almost complete protection against cytokines, in keeping with previous reports of protection by NOS inhibitors (*4*, *8*). Our results, moreover, provide some new insights into the mechanisms of S-nitrosylation in vivo and the metabolic fate of endogenous RNS.

In particular, RNS-induced apoptosis can be broadly classified as either nitrosative or oxidative in nature; that is, ultimately, RNS will either oxidize or nitros(yl)ate (*35*, *40*, *51*, *60*). Among RNS, peroxynitrite has been closely identified with oxidation (*61*) and GSNO with nitrosation (*41*), when in fact NO/O_2^- interactions can result in nitrosative chemistry under some conditions. Bioassays by us here and others (*6*) reveal that RAW 264.7 cells are relatively resistant to combinations of NO/O_2^- (peroxynitrite-related molecules) but quite sensitive to nitrosants such as GSNO. We further show that superoxide production does not significantly impact the level of nitros(yl)ation, but is associated with higher nitrate to nitrite yields. These results are consistent with the picture of macrophages relatively impervious to oxidants (*29*) and with a mechanism in which superoxide diverts NO away from nitrosative pathways (*33*, *51*)—which appear to activate the cell death program—toward peroxynitrite-related species which are apparently well handled (*29*) by constitutive cellular defenses, such as glutathione peroxidase (*62*), and tend to yield nitrate. The data also indicate that the reactive pathways available to S-nitrosylate proteins (*33*, *51*, *63*) in RAW cells are probably independent of ROS and distinct from those that yield nitrite and nitrate, as seemed to be the case in human airway-lining fluid (*64*).

Analysis of the fate of RNS synthesized by activated macrophages reveals that the ratio of nitrate to nitrite (a marker for oxidation) fell coincident with the onset of nitrosation reactions (evidenced by diazotization of DAN at physiologic pH and an increased rate of nitrite production) (Figures 1C,D and 3A). In other words, the expression of oxidative and nitrosative stresses is sequentially regulated. That DAN, which competes relatively poorly with intracellular glutathione and nucleophilic sites in proteins, was nevertheless nitrosated suggests that cells are subjected to considerable stress. Indeed, contemporaneous analyses revealed extensive nitrosylation of proteins. That is, ~1% of protein was modified during steady-state NO synthesis (during which no major change in cellular redox state was detected). The case for a causal linkage between nitrosylation and apoptosis is strengthened by the qualitative and quantitative similarities in effects of endogenous RNS and exogenous GSNO. Specifically, RNS and GSNO produced comparable amounts of cell death and levels of nitros(yl)ation. Lewis and colleagues have previously found that RNS generation by macrophages coincided with nitrosation of amines, but that the rate of nitrosamine formation was 6-fold lower than predicted (*30*). They concluded that additional intracellular substrates must be preferentially nitros(yl)ated. Thiols in peptides and proteins are much more reactive than biological amines (*65*, *66*). Thus, our results are in keeping with the known order of bimolecular reactivity (thiol > amine) and the predictions of Lewis et al. (*30*). They are also in agreement with work by Geng et al., who detected high levels of nitrosylated proteins with electron paramagnetic resonance, in cells undergoing apoptosis (*67*).

That GSNO did not accumulate intracellularly strongly suggests that it is metabolized. Indeed, an emerging picture in NO biology is of a ubiquitous metabolism for SNOs that may subserve cell-specific functions (*40*, *68*−*71*). A tightly regulated GSNO detoxification pathway in *E. coli* may be relevant to this case (*40*). The bacterium has constitutive activities that cleave SNO to NO (and perhaps other RNS) and an inducible flavohemoprotein, which then oxidizes NO to nitrate and nitrite (*72*, *73*). Moreover, molecular recognition of such a nitrosative stress is partly achieved through formation of SNO in proteins, whose function is the induction of genes controlling nitrosant metabolism (*40*). One might speculate that similar adaptive mechanisms exist to alleviate a nitrosative challenge in macrophages—lysates of which contain a constitutive NO consumption activity (*74*). Nitrosylation may also serve directly in cellular defenses. For example, S-nitrosylation of caspases may function as a counter-regulatory (protective) posttranslational modification (*36*, *75*−*77*), and glutathione nitrosylation (*64*, *70*, *78*) may buffer against DNA deamination, thereby protecting from cell death (*54*, *79*−*81*). Caspases were, in fact, activated by INF-γ/LPS treatment in our studies, but the activity was kept at very low levels (data not shown).

Oxidation and nitrosation are not mutually exclusive events. Cells challenged by nitrosative stress may be subject to a concomitant oxidative threat (*35*, *40*, *60*, *82*). Moreover, a continuum exists between nitrosation and oxidation in biological systems. That is, high concentrations of nitrosants engender oxidation (*35*). In some cases, nitrosation and oxidation may synergize to elicit the response (as in the antimicrobial actions of ROS and RNS) (*83*). In other instances, redox responsiveness may involve one class of nitrosant or oxidant molecule or depend on a singular type of protein modification. It would appear that p53-induced apoptosis of INF-γ/LPS-activated murine macrophages falls into the latter category; that is, the principle mechanism is nitrosative. Inasmuch as this model typifies iNOS-mediated cellular injury, nitrosative stress may be widely involved in NO pathogenesis.

REFERENCES

1. Nathan, C. (1992) *FASEB J. 6*, 3051−3064.
2. Messmer, U. K., Ankarcrona, M., Nicotera, P., and Brune, B. (1994) *FEBS Lett. 355*, 23−26.
3. Messmer, U. K., Reed, U. K., and Brune, B. (1996) *J. Biol. Chem. 271*, 20192−20197.
4. Messmer, U. K., Reimer, D. M., Reed, J. C., and Brune, B. (1996) *FEBS Lett. 384*, 162−166.
5. Messmer, U. K., and Brune, B. (1996) *Arch. Biochem. Biophys. 327*, 1−10.
6. Messmer, U. K., Lapetina, E. G., and Brune, B. (1995) *Mol. Pharmacol. 47*, 757−765.
7. Messmer, U. K., and Brune, B. (1996) *Biochem. J. 319*, 299−305.
8. Sarih, M., Souvannavong, V., and Adam, A. (1993) *Biochem. Biophys. Res. Commun. 191*, 503−508.
9. Zhuang, J. C., and Wogan, G. N. (1997) *Proc. Natl. Acad. Sci. U.S.A. 94*, 11875−11880.
10. Fehsel, K., Kroncke, K. D., Meyer, K. L., Huber, H., Wahn, V., and Kolb-Bachofen, V. (1995) *J. Immunol. 155*, 2858−2865.
11. Cui, S., Reichner, J. S., Mateo, R. B., and Albina, J. E. (1994) *Cancer Res. 54*, 2462−2467.
12. Ischiropoulos, H., Zhu, L., and Beckman, J. S. (1992) *Arch. Biochem. Biophys. 298*, 446−451.
13. Lotem, J., Peled-Kamar, M., Groner, Y., and Sachs, L. (1996) *Proc. Natl. Acad. Sci. U.S.A. 93*, 9166−9171.
14. Kaul, N., Gopalakrishna, R., Gundimeda, U., Choi, J., and Forman, H. J. (1998) *Arch. Biochem. Biophys. 350*, 79−86.
15. Xia, Y., and Zweier, J. L. (1997) *Proc. Natl. Acad. Sci. U.S.A. 94*, 6954−6958.
16. Vazquez-Torres, A., Jones-Carson, J., and Balish, E. (1996) *Infect. Immun. 64*, 3127−3133.
17. Yin, Y., Terauchi, Y., Solomon, G. G., Aizawa, S., Rangarajan, P. N., Yazaki, Y., Kadowaki, T., and Barrett, J. C. (1998) *Nature 391*, 707−710.
18. Polyak, K., Xia, Y., Zweier, J. L., Kinzler, K. W., and Vogelstein, B. (1997) *Nature 389*, 300−305.
19. Johnson, T. M., Yu, Z. X., Ferrans, V. J., Lowenstein, R. A., and Finkel, T. (1996) *Proc. Natl. Acad. Sci. U.S.A. 93*, 11848−11852.
20. Jacobson, M. D. (1996) *Trends Biochem. Sci. 21*, 83−86.
21. Hockenbery, D. M., Oltvai, Z. N., Yin, X. M., Milliman, C. L., and Korsmeyer, S. J. (1993) *Cell 75*, 241−251.
22. Kane, D. J., Sarafian, T. A., Anton, R., Hahn, H., Gralla, E. B., Valentine, J. S., Ord, T., and Bredesen, D. E. (1993) *Science 262*, 1274−1277.
23. Bonfoco, E., Krainc, D., Ankarcrona, M., Nicotera, P., and Lipton, S. A. (1995) *Proc. Natl. Acad. Sci. U.S.A. 92*, 7162−7166.
24. Cai, J., and Jones, D. P. (1998) *J. Biol. Chem. 273*, 11401−11404.
25. Lin, K. T., Xue, J. Y., Nomen, M., Spur, B., and Wong, P. Y. (1995) *J. Biol. Chem. 270*, 16487−16490.
26. Kaul, N., Choi, J., and Forman, H. J. (1998) *Free Radical Biol. Med. 24*, 202−207.
27. Steinman, H. M. (1995) *J. Biol. Chem. 270*, 3487−3490.
28. Clement, M. V., and Stamenkovic, I. (1996) *EMBO J. 15*, 216−225.
29. Brune, B., Gotz, C., Messmer, U. K., Sandau, K., Hirvonen, M. R., and Lapetina, E. G. (1997) *J. Biol. Chem. 272*, 7253−7258.

30. Lewis, R. S., Tamir, S., Tannenbaum, S. R., and Deen, W. M. (1995) *J. Biol. Chem. 270*, 29350−29355.
31. Kobayashi, T., Robinson, J. M., and Seguchi, H. (1998) *J. Cell Sci. 111*, 81−91.
32. Nunoshiba, T., deRojas-Walker, T., Wishnok, J. S., Tannenbaum, S. R., and Demple, B. (1993) *Proc. Natl. Acad. Sci. U.S.A. 90*, 9993−9997.
33. Stamler, J. S. (1994) *Cell 78*, 931−936.
34. Stamler, J. S., Toone, E. J., Lipton, S. A., and Sucher, N. J. (1997) *Neuron 18*, 691−696.
35. Stamler, J. S., and Hausladen, A. (1998) *Nat. Struct. Biol. 5*, 247−249.
36. Melino, G., Bernassola, F., Knight, R. A., Corasaniti, M. T., Nistico, G., and Finazzi-Agro, A. (1997) *Nature 388*, 432−433.
37. Jia, L., Bonaventura, C., Bonaventura, J., and Stamler, J. S. (1996) *Nature 380*, 221−226.
38. Kobzik, L., Reid, M. B., Bredt, D. S., and Stamler, J. S. (1994) *Nature 372*, 546−548.
39. Eu, J. P., Xu, L., Stamler, J. S., and Meissner, G. (1999) *Biochem. Pharmacol. 57*, 1079−1084.
40. Hausladen, A., Privalle, C. T., Keng, T., DeAngelo, J., and Stamler, J. S. (1996) *Cell 86*, 719−729.
41. Stamler, J. S., and Feelisch, M. (1996) in *Methods in Nitric Oxide Research* (Feelisch, M., and Stamler, J. S., Eds.) pp 521−539, John Wiley & Sons Ltd., Chichester, U.K.
42. Hill, J. R., Corbett, J. A., Kwon, G., Marshall, C. A., and McDaniel, M. L. (1996) *J. Biol. Chem. 271*, 22672−22678.
43. Misko, T. P., Schilling, R. J., Salvemini, D., Moore, W. M., and Currie, M. G. (1993) *Anal. Biochem. 214*, 11−16.
44. Andrew, P. J., Auer, M., Lindley, I. J., Kauffmann, H. F., and Kungl, A. J. (1997) *FEBS Lett. 408*, 319−323.
45. Kosower, N. S., and Kosower, E. M. (1987) *Methods Enzymol. 143*, 264−270.
46. Griffith, O. W. (1980) *Anal. Biochem. 106*, 207−212.
47. Vassault, A. (1983) in *Methods of Enzymatic Analysis* (Bergmeyer, H. U., Ed.) pp 118−126, Academic Press, New York.
48. Wang, J. F., Komarov, P., and de Groot, H. (1993) *Arch. Biochem. Biophys. 304*, 189−196.
49. Kim, Y. M., de Vera, M. E., Watkins, S. C., and Billiar, T. R. (1997) *J. Biol. Chem. 272*, 1402−1411.
50. Farias-Eisner, R., Chaudhuri, G., Aeberhard, E., and Fukuto, J. M. (1996) *J. Biol. Chem. 271*, 6144−6151.
51. Wink, D. A., Cook, J. A., Kim, S. Y., Vodovotz, Y., Pacelli, R., Krishna, M. C., Russo, A., Mitchell, J. B., Jourd'heuil, D., Miles, A. M., and Grisham, M. B. (1997) *J. Biol. Chem. 272*, 11147−11151.
52. Wink, D. A., Cook, J. A., Krishna, M. C., Hanbauer, I., DeGraff, W., Gamson, J., and Mitchell, J. B. (1995) *Arch. Biochem. Biophys. 319*, 402−407.
53. Rubbo, H., Radi, R., Trujillo, M., Telleri, R., Kalyanaraman, B., Barnes, S., Kirk, M., and Freeman, B. A. (1994) *J. Biol. Chem. 269*, 26066−26075.
54. Burney, B., Tamir, S., Aaron, G., and Tannenbaum, S. R. (1997) *Nitric Oxide: Biol. Chem. 1*, 130−144.
55. Hiraoka, W., Vazquez, N., Nieves-Neira, W., Chanock, S. J., and Pommier, Y. (1998) *J. Clin. Invest. 102*, 1961−1968.
56. Day, B. J., Patel, M., Calavetta, L., Chang, L. Y., and Stamler, J. S. (1999) *Proc. Natl. Acad. Sci. U.S.A. 96*, 12760−12765.
57. van den Dobbelsteen, D. J., Nobel, C. S. I., Schlegel, J., Cotgreave, I. A., Orrenius, S., and Slater, A. F. (1996) *J. Biol. Chem. 271*, 15420−15427.
58. Banki, K., Hutter, E., Colombo, E., Gonchoroff, N. J., and Perl, A. (1996) *J. Biol. Chem. 271*, 32994−33001.
59. Beaver, J. P., and Waring, P. (1995) *Eur. J. Cell. Biol. 68*, 47−54.
60. Becker, K., Savvides, S. N., Keese, M., Schirmer, R. H., and Karplus, P. A. (1998) *Nat. Struct. Biol. 5*, 267−271.
61. Pryor, W. A., and Squadrito, G. L. (1995) *Am. J. Physiol. 268*, L699−722.
62. Sies, H., Sharov, V. S., Klotz, L. O., and Briviba, K. (1997) *J. Biol. Chem. 272*, 27812−27817.
63. Gow, A. J., Luchsinger, B. P., Pawloski, J. R., Singel, D. J., and Stamler, J. S. (1999) *Proc. Natl. Acad. Sci. U.S.A. 96*, 9027−9032.
64. Gaston, B., Reilly, J., Drazen, J. M., Fackler, J., Ramdev, P., Arnelle, D., Mullins, M. E., Sugarbaker, D. J., Chee, C., Singel, D. J., et al. (1993) *Proc. Natl. Acad. Sci. U.S.A. 90*, 10957−10961.
65. Wink, D. A., Nims, R. W., Darbyshire, J. F., Christodoulou, D., Hanbauer, I., Cox, G. W., Laval, F., Laval, J., Cook, J. A., Krishna, M. C., et al. (1994) *Chem. Res. Toxicol. 7*, 519−525.
66. Simon, D. I., Mullins, M. E., Jia, L., Gaston, B., Singel, D. J., and Stamler, J. S. (1996) *Proc. Natl. Acad. Sci. U.S.A. 93*, 4736−4741.
67. Geng, Y.-J., Hellstrand, K., Wennmalm, A., and Hansson, G. (1996) *Cancer Res. 56*, 866−874.
68. Gordge, M. P., Addis, P., Noronha-Dutra, A. A., and Hothersall, J. S. (1998) *Biochem. Pharmacol. 55*, 657−665.
69. Mayer, B., Pfeiffer, S., Schrammel, A., Koesling, D., Schmidt, K., and Brunner, F. (1998) *J. Biol. Chem. 273*, 3264−3270.
70. Akaike, T., Inoue, K., Okamoto, T., Nishino, H., Otagiri, M., Fujii, S., and Maeda, H. (1997) *J. Biochem. 122*, 459−466.
71. Gaston, B., Sears, S., Woods, J., Hunt, J., Ponaman, M., McMahon, T., and Stamler, J. S. (1998) *Lancet 351*, 1317−1319.
72. Gardner, P. G., Gardner, A. M., Martin, L. A., and Salzman, A. L. (1998) *Proc. Natl. Acad. Sci. U.S.A. 95*, 10378−10383.
73. Hausladen, A., Gow, A. J., and Stamler, J. S. (1998) *Proc. Natl. Acad. Sci. U.S.A. 95*, 14100−14105.
74. Liu, L., Zeng, M., and Stamler, J. S. (1999) *Proc. Natl. Acad. Sci. U.S.A. 96*, 6643−6647.
75. Dimmeler, S., Haendeler, J., Nehls, M., and Zeiher, A. M. (1997) *J. Exp. Med. 185*, 601−607.
76. Kim, Y. M., Talanian, R. V., and Billiar, T. R. (1997) *J. Biol. Chem. 272*, 31138−31148.
77. Mannick, J. B., Miao, X. Q., and Stamler, J. S. (1997) *J. Biol. Chem. 272*, 24125−24128.
78. Hogg, N., Singh, R. J., and Kalyanaraman, B. (1996) *FEBS Lett. 382*, 223−228.
79. Nguyen, T., Brunson, D., Crespi, C. L., Penman, B. W., Wishnok, J. S., and Tannenbaum, S. R. (1992) *Proc. Natl. Acad. Sci. U.S.A. 89*, 3030−3034.
80. Walker, M. W., Kinter, M. T., Roberts, R. J., and Spitz, D. R. (1995) *Pediatr. Res. 37*, 41−49.
81. Tu, B., Wallin, A., Moldeus, P., and Cotgreave, I. (1995) *Toxicology 98*, 125−136.
82. Poderoso, J. J., Carreras, M. C., Lisdero, C., Riobo, N., Schopfer, F., and Boveris, A. (1996) *Arch. Biochem. Biophys. 328*, 85−92.
83. Fang, F. C. (1997) *J. Clin. Invest. 100*, S43−S50.

BI992046E